



Age, origin and significance of a new middle MIS 3 tephra horizon identified within a long-core sequence from Les Echets, France

DANIEL VERES, SIWAN M. DAVIES, BARBARA WOHLFARTH, FRANK PREUSSER, STEFAN WASTEGÅRD, LINDA AMPEL, ANNE HORMES, GÖRAN POSSNERT, JEAN-PAUL RAYNAL AND GÉRARD VERNET

BOREAS

Veres, D., Davies, S. M., Wohlfarth, B., Preusser, F., Wastegård, S., Ampel, L., Hormes, A., Possnert, G., Raynal, J.-P. & Vernet, G. 2008 (August): Age, origin and significance of a new middle MIS 3 tephra horizon identified within a long-core sequence from Les Echets, France. *Boreas*, Vol. 37, pp. 434–443. 10.1111/j.1502-3885.2008.00028.x. ISSN 0300-9483.

A new tephra has been identified within a long core (EC 3) sequence recovered from Les Echets, near Lyon, France. This visible tephra was discovered as part of a high resolution multiproxy re-investigation of the Les Echets sequence. Independent chronological information suggests that the tephra is *c.* 42 000–45 000 years old, and geochemical analysis indicates that it is of basanitic composition. The latter suggests a possible origin in the Eifel; however, as yet, no other volcanic events or deposits can be correlated to the Les Echets tephra. New sedimentological and chronological data are presented indicating that the tephra falls within an interval that most likely correlates with Dansgaard–Oeschger events 12–9. Thus, this tephra could potentially be an important middle MIS 3 marker horizon in central Europe if it can be traced in other palaeorecords.

Daniel Veres (e-mail: danveres@hasdeu.ubbcluj.ro), 'Emil Racovita' Speleological Institute, Clinicilor 5, 400006 Cluj, Romania and Stockholm University, Department of Physical Geography and Quaternary Geology, SE-10691 Stockholm, Sweden; Siwan M. Davies, School of the Environment and Society, University of Wales Swansea, Singleton Park, Swansea SA2 8PP, Wales, UK; Barbara Wohlfarth, Department of Geology and Geochemistry, SE-10691 Stockholm, Sweden; Frank Preusser, Institut für Geologie, Universität Bern, Baltzerstrasse 1+3, 3012 Bern, Switzerland; Stefan Wastegård and Linda Ampel, Stockholm University, Department of Physical Geography and Quaternary Geology, SE-10691 Stockholm, Sweden; Anne Hormes, Quaternary Geology, The University Centre in Svalbard, P.O. Box 156, NO-9171 Longyearbyen, Norway; Göran Possnert, Ångströmlaboratory, Uppsala University, P.O. Box 534, SE-75121 Uppsala, Sweden; Jean-Paul Raynal, CNRS UMR 5199 PACEA, Université de Bordeaux I, IPGQ, Avenue des facultés, F-33405 Talence, France; Gérard Vernet, CNRS UMR 6042, NRAP, rue du Mont Mouchet 7, F-63320 Chadeleuf, France; received 20th July 2007, accepted 23rd February 2008.

The long-sedimentary sequence at Les Echets (45°54'N; 4°56'E) (Fig. 1) was first investigated by de Beaulieu & Reille (1984), whose work showed that Les Echets is one of the few terrestrial sequences in Europe that provided detailed insight into vegetation changes during the last glacial cycle. Alternating phases of forest and open vegetation during Marine Isotope Stage (MIS) 5 and a dominance of cold-tolerant species (MIS 4–2) are some of the key changes that have been identified (de Beaulieu & Reille 1984). Moreover, the detailed pollen stratigraphy has shown that pine pollen percentages fluctuated in a quasi-cyclic pattern throughout most of MIS 3. These fluctuations in pine pollen are of particular importance and may be responding to rapid climate oscillations – the so-called Dansgaard–Oeschger (DO) events – identified in the ice-core records during the last glacial period (Johnsen *et al.* 1992; Dansgaard *et al.* 1993). Although evidence for these millennial-scale fluctuations has been identified in a number of different palaeoarchives in Europe (e.g. Allen *et al.* 1999; Sánchez Goñi *et al.* 2002; Spötl & Mangini 2002; Genty *et al.* 2003), an understanding of the spatial variability and, in particular, of the nature of the terrestrial response to these events is still incomplete. Accordingly, the need to address these questions was the main impetus for carrying out a new multiproxy investigation of the Les Echets sequence. Not only does

this site offer a high-resolution record of environmental changes during the late Quaternary (Veres *et al.* 2007), but in particular its location, in an intermediate position between central northern Europe and the Mediterranean region (Fig. 1A), could add important data determining the spatial variability and impact of these rapid climatic fluctuations in Europe.

New sediment cores were obtained from the centre (EC 1) and margin (EC 3) of the basin in 2001 (Fig. 1B). Good chronological control of the analysed sediment sequences has been a central component of this project with the employment of three different dating methods – radiocarbon dating, luminescence dating and tephrochronology. The last-mentioned, in particular, offers considerable potential for the precise correlation between different archives, particularly as recent work has demonstrated that volcanic ash from some events can be traced over areas far more distal than previously realized (e.g. Davies *et al.* 2003; Hang *et al.* 2006; Pyle *et al.* 2006; Blockley *et al.* 2007). The site of Les Echets has the potential for preserving a record of volcanic events from a number of different European sources during the last glacial period (Fig. 1A). In particular, this site is ideally located for establishing a record of intra-plate volcanism from the nearby Massif Central and the more distal Eifel volcanic field in Germany (Fig. 1A). Recent work suggests that Quaternary

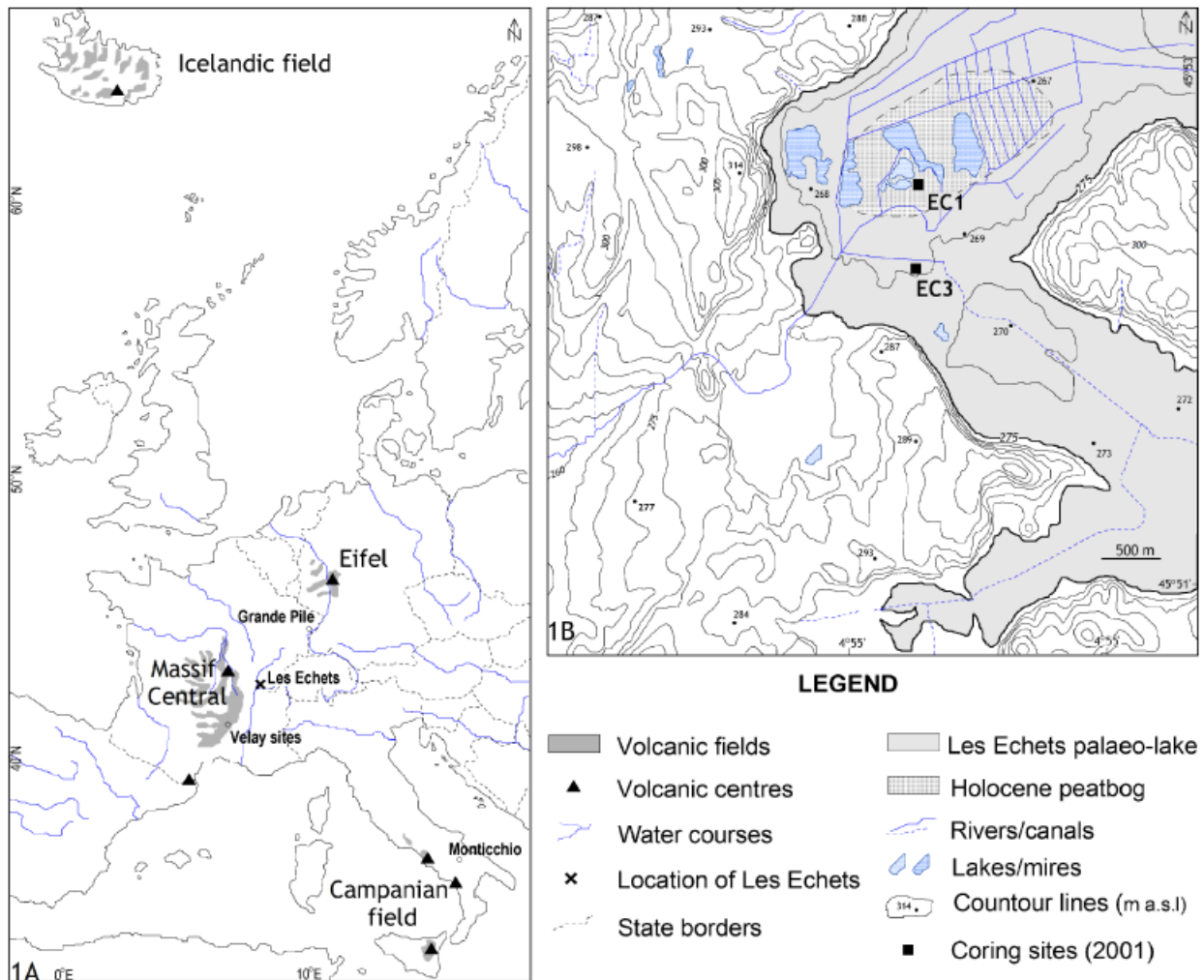


Fig. 1. A. The location of Les Echets and its geographical relation to the main late Pleistocene volcanic centres of Europe. B. Detailed topographic map over the western part of the Les Echets mire and the location of the cores recovered in 2001 (adapted from Veres *et al.* 2007).

volcanism in these regions is episodic, correlating in particular with warming at the beginning of interglacial periods (Nowell *et al.* 2006). During the last glacial period, however, a number of volcanic events are known to have occurred in these regions. Volcanism in the Massif Central occurred predominantly along the Chaîne des Puys, with at least 75 ash-fall events identified in the Clermont Ferrand basin (Vernet *et al.* 1998). In the Eifel region, on the other hand, the frequency of volcanic events is lower during the glacial period (Nowell *et al.* 2006), although some are thought to have been high magnitude eruptions, e.g. Meerfelder Maar (Zolitschka *et al.* 1995; Schmincke *in press*).

Here we report on the identification of the first tephra horizon in the marginal core EC 3 (<14.55 m depth) from Les Echets spanning MIS 3 and MIS 2. New luminescence and radiocarbon age determinations are used to develop a chronological model and an age estimate for the tephra horizon. New sedimentological data are also presented to provide a palaeoenvironmental and palaeoclimatic context (MIS 3 and 2) for

this tephra horizon. These new data build on the data published previously in Veres *et al.* (2007).

Methods

Tephra and mineralogical analyses

Sampling for tephra was initially undertaken on 25 cm long contiguous samples which contained a number of coarse-grained layers. These samples were prepared according to the methodology outlined in Turney (1998) and Davies *et al.* (2005) for the preparation of minerogenic lake sediments. Subsequent to ashing and sieving the material, density separation (using SPT, sodium polytungstate [$\text{Na}_6(\text{H}_2\text{W}_{12}\text{O}_{40})\text{H}_2\text{O}$]) was undertaken to separate the material at 2.5 g cm^{-3} . The $<2.5 \text{ g cm}^{-3}$ material was subsequently subjected to a NaOH treatment to remove the biogenic silica (Rose *et al.* 1996). Identification of tephra shards was undertaken optically using a high-magnification light microscope. This procedure was repeated

Table 1. Electron microprobe analysis of glass shards for the tephra identified at 10.86 m in core EC 3. Operating conditions of the Cameca SX 100 electron microprobe are as follows: accelerating voltage 15 kV, beam current 10 nA, beam diameter rastered over 10 μm . Counting times on the peak of each element was restricted to 10 s. Sodium was measured in the first counting period and a series of standards (pure metals, synthetic oxides and silicates) was used for calibration. Any drift in the reading was monitored by analysing an andradite at regular intervals. A PAP correction was applied for atomic number, absorption and fluorescence effects (Pouchou & Pichoir 1991).

| n | SiO ₂ | TiO ₂ | Al ₂ O ₃ | FeO | MnO | MgO | CaO | Na ₂ O | K ₂ O | P ₂ O ₅ | Total |
|----------|------------------|------------------|--------------------------------|-------|------|------|-------|-------------------|------------------|-------------------------------|-------|
| 1 | 44.38 | 3.24 | 15.79 | 10.89 | 0.19 | 4.92 | 11.11 | 5.31 | 2.44 | 1.08 | 99.35 |
| 2 | 44.52 | 3.31 | 15.67 | 10.85 | 0.20 | 4.98 | 11.16 | 5.17 | 2.36 | 1.10 | 99.31 |
| 3 | 44.38 | 3.36 | 15.72 | 10.92 | 0.19 | 4.45 | 11.20 | 5.40 | 2.29 | 1.07 | 98.97 |
| 4 | 44.00 | 3.18 | 15.69 | 11.06 | 0.18 | 5.52 | 10.57 | 5.40 | 2.31 | 1.04 | 98.95 |
| 5 | 43.89 | 3.14 | 15.84 | 11.01 | 0.23 | 4.86 | 11.22 | 5.42 | 2.27 | 1.05 | 98.92 |
| 6 | 44.09 | 3.28 | 15.73 | 10.96 | 0.24 | 5.12 | 10.97 | 5.09 | 2.24 | 1.04 | 98.77 |
| 7 | 44.15 | 3.26 | 15.75 | 10.89 | 0.16 | 4.95 | 10.89 | 5.29 | 2.36 | 1.07 | 98.77 |
| 8 | 43.95 | 3.35 | 15.48 | 10.85 | 0.16 | 5.10 | 11.26 | 5.15 | 2.31 | 1.02 | 98.63 |
| 9 | 44.72 | 3.26 | 15.73 | 10.48 | 0.15 | 4.43 | 10.94 | 5.43 | 2.37 | 1.09 | 98.60 |
| 10 | 43.85 | 3.31 | 15.85 | 10.63 | 0.20 | 4.74 | 10.99 | 5.44 | 2.32 | 1.03 | 98.37 |
| 11 | 43.82 | 3.17 | 15.66 | 10.65 | 0.21 | 5.20 | 10.97 | 5.15 | 2.43 | 1.03 | 98.30 |
| 12 | 43.50 | 3.24 | 15.43 | 11.08 | 0.23 | 5.08 | 11.03 | 5.28 | 2.35 | 1.02 | 98.25 |
| 13 | 43.90 | 3.18 | 15.97 | 10.47 | 0.18 | 4.65 | 11.01 | 5.42 | 2.39 | 1.06 | 98.23 |
| 14 | 44.19 | 3.19 | 15.42 | 10.61 | 0.22 | 4.97 | 10.98 | 5.31 | 2.25 | 1.07 | 98.21 |
| 15 | 44.06 | 3.22 | 15.54 | 10.71 | 0.17 | 4.84 | 11.10 | 5.11 | 2.34 | 1.05 | 98.13 |
| 16 | 43.61 | 3.21 | 15.69 | 10.82 | 0.17 | 4.99 | 10.96 | 5.22 | 2.39 | 1.07 | 98.11 |
| 17 | 44.19 | 3.27 | 15.67 | 10.73 | 0.21 | 4.44 | 10.77 | 5.35 | 2.38 | 1.08 | 98.09 |
| 18 | 43.52 | 3.14 | 15.57 | 10.83 | 0.19 | 4.98 | 11.03 | 5.41 | 2.37 | 1.02 | 98.05 |
| 19 | 44.24 | 2.78 | 15.79 | 9.97 | 0.18 | 4.46 | 10.96 | 5.83 | 2.43 | 0.96 | 97.57 |
| 20 | 42.25 | 3.18 | 15.49 | 10.69 | 0.23 | 4.31 | 10.88 | 5.29 | 2.38 | 0.99 | 95.68 |
| Mean | 43.96 | 3.21 | 15.67 | 10.75 | 0.19 | 4.85 | 11.00 | 5.32 | 2.35 | 1.05 | 98.36 |
| St. dev. | 0.51 | 0.12 | 0.15 | 0.25 | 0.03 | 0.31 | 0.16 | 0.16 | 0.06 | 0.04 | 0.78 |

at a 1 cm sampling resolution if tephra shards were identified to pinpoint precisely the position of the tephra within the 25 cm long subsample. Where low concentrations of basaltic material were identified within the $<2.5 \text{ g cm}^{-3}$ fraction, further investigation of the $>2.5 \text{ g cm}^{-3}$ fraction was also undertaken with a light microscope. Geochemical analysis of glass shards was done on a SX-100 Cameca electron microprobe at the Tephrochronology Analytical Unit, University of Edinburgh. Operating conditions are outlined in Table 1. During microprobe analysis, inclusions within the glass shards were avoided so as not to affect the geochemical composition of the glass itself.

For analysis of the minerals found in association with the tephra, two fractions (250–160 μm and 125–80 μm) were isolated and observed under a petrological microscope. Particle-size distribution of bulk tephra, as well as of the two magnetically separated fractions, was measured by hand sieving (Fig. 2). The magnetic separation was performed on a Franz Magnetic Separator model L-1 following the methodology outlined in Mackie *et al.* (2002).

Infrared stimulated luminescence dating

For infrared stimulated luminescence (IRSL) dating, the polymineral fine grain fraction (4–11 μm) of the inner part (not exposed to sunlight) of the half-cores was extracted after chemical pretreatments (HCl, H₂O₂, Na-Oxalate) by settling using Stokes' law. The silt fraction was used because this fraction dominated in

the sediments of core EC 3. We did not attempt to extract the quartz fraction from the samples, because this mineral usually has poor luminescence properties in samples investigated from the Alpine region (Klasen *et al.* 2006; Preusser *et al.* 2006). Previous experience reveals that K-feldspars, which will dominate the investigated IRSL signal from polymineral fine grains, are a reliable natural dosimeter in the Alpine realm (e.g. Preusser 2003; Preusser *et al.* 2003; Preusser & Schlüchter 2004) despite the problems observed for this mineral in some other areas.

Determination of D_e was carried out using the modified single-aliquot regenerative-dose (SAR) protocol of Preusser (2003) on a Risø TL/OSL reader. The detection filter was a combination of a Schott BG-39, a Schott GG400 and a Corning 7-59 giving a peak emission at $\sim 410 \text{ nm}$. IRSL was recorded during a 300 s shine-down of IR diodes. The integral 200–300 s was subtracted from the rest of the IRSL decay curves as late light, and the signal of the first 5 s was used for constructing dose–response curves. A preheat temperature of 290 °C and a cut heat of 200 °C were applied. This procedure was cross-checked by preheat and dose–recovery tests, applying a dose of the same magnitude as the natural dose. The average ratio of applied/regenerated dose for the investigated samples is 1.04 ± 0.07 . All samples showed recycling ratios close to 1.00 and low recuperation (3–4%). This proves the good performance of the applied measurement procedure. Seven aliquots were measured for each sample. The plot of D_e versus stimulation time shows a flat

Table 2. AMS ^{14}C measurements for core EC 3. The 'calibrated' ages were calculated according to Fairbanks *et al.* (2005) on-line calibration programme. The modern ages obtained around 1.20 m depth indicate that either the dated material (twigs) has been introduced into the sediment during coring or the sediment has been disturbed by agricultural activities.

| Laboratory number | Depth (cm) | Material | ^{14}C ages yr BP ($\pm 1\sigma$) | $\delta^{13}\text{C}$ (‰ PDB) | Cal ages yr BP ($\pm 1\sigma$) |
|-------------------|------------|-----------------------|--|-------------------------------|----------------------------------|
| Ua 17109 | 120 | Wood fragments | Modern | -27.5 | |
| Ua 17110 | 123 | Wood fragments | Modern | -31.1 | |
| Poz 2494 | 488–498 | Organic detritus | 23 640 \pm 150 | – | 28 190 \pm 180 |
| LuS 6150 | 510–511.5 | <i>Phragmites</i> sp. | 24 140 \pm 120 | – | 28 718 \pm 149 |
| LuS 6181 | 548 | <i>Phragmites</i> sp. | 24 300 \pm 140 | – | 28 887 \pm 166 |
| LuS 6182 | 775 | <i>Phragmites</i> sp. | 29 470 \pm 230 | – | 34 634 \pm 403 |
| LuS 6351 | 1082–1083 | Bulk sediment | 42 000 \pm 1000 | – | 45 686 \pm 912 |
| LuS 6350 | 1088–1089 | Bulk sediment | 36 600 \pm 500 | – | 41 723 \pm 310 |
| LuS 6183 | 1115 | Organic detritus | 37 370 \pm 550 | – | 42 177 \pm 336 |
| LuS 5993 | 1134 | Organic detritus | 37 385 \pm 830 | – | 42 195 \pm 534 |
| Ua 17111 | 1152 | <i>Phragmites</i> sp. | 38 480 \pm 490 | -16.2 | 42 890 \pm 422 |
| Ua 16751 | 1253–1254 | <i>Phragmites</i> sp. | >41000 | -13.5 | |
| Ua 16860 | 1775–1776 | Aquatic mosses | >41000 | -27.9 | |

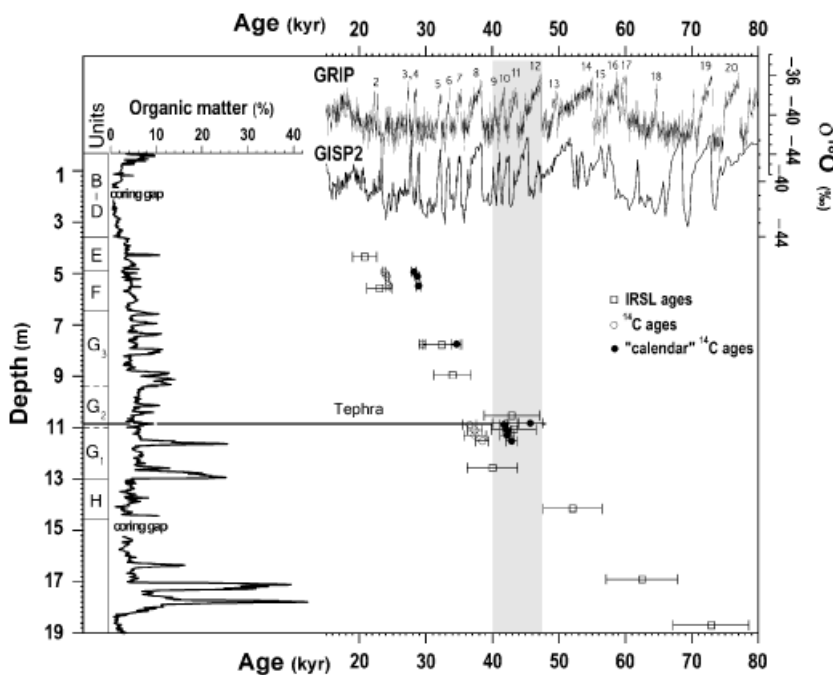


Fig. 3. IRSL, AMS ^{14}C and 'calibrated' AMS ^{14}C dates plotted versus depth for core EC 3. The ^{14}C ages are plotted with two sigma error and the IRSL ages with one sigma error. Lithostratigraphic units are also shown and the horizontal line indicates the position of the tephra layer discussed in the text. The vertical grey bar suggests the most likely time interval when the tephra was deposited. The organic matter contents of core EC 3 and the $\delta^{18}\text{O}_{\text{ice}}$ records from the GRIP (Johnsen *et al.* 2001) and GISP2 (Meese *et al.* 1997) ice-cores are shown for comparison. Numbers 2–20 refer to Dansgaard–Oeschger (DO) interstadials.

sample (2 cm increments) at 105 °C for 24 h, followed by combustion for 4 h at 550 °C and 925 °C, respectively. The minerogenic content represents the ignition residue after combusting the samples at 925 °C (Fig. 4). All parameters are given as percentage (%) loss of the original weight (Heiri *et al.* 2001). Dry density was calculated as the dry mass of the sample divided by its wet volume and is expressed as g cm^{-3} .

Particle-size distribution was determined by laser diffraction using a Fritsch A22 Laser Particle Sizer. Sample preparation and measurement details are given in Konert & Vandenberghe (1997). The cumulative particle-size distribution is reported as total sand fraction (63 μm – 2 mm), total silt fraction (5.5–63 μm) and total clay fraction (<5.5 μm).

Whole core magnetic susceptibility was measured on split half-cores with a Bartington MS2EI point sensor core logger at 0.5 cm resolution. The susceptibility meter operated at 0.565 kHz, with a low field intensity of 80 A/m.

Results and discussion

Geochemical and mineralogical characterization of the tephra

A high concentration of dark brown glass shards was identified within the $>2.5 \text{ g cm}^{-3}$ fraction at 10.86 m in core EC 3, relating to a visible coarse-grained layer *c.* 5 mm thick. A peak in magnetic susceptibility also

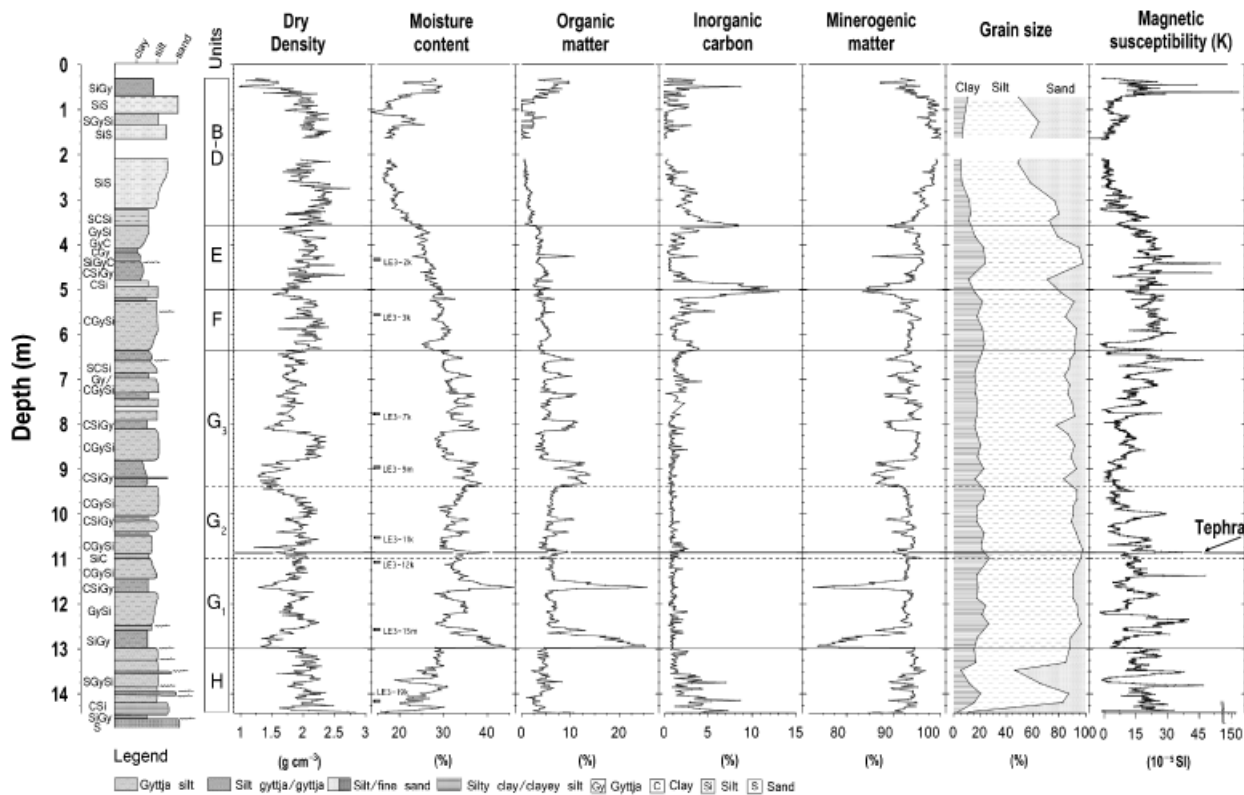


Fig. 4. Lithostratigraphy and vertical profiles of dry density, moisture, organic matter content, inorganic carbon, minerogenic content, grain-size variations and magnetic susceptibility (K) between 14.55 and 0.30 m depth in core EC 3. A thin (0.5 cm) tephra layer discussed in the text is indicated by the horizontal line and by an arrow in the magnetic susceptibility graph. Horizontal dashed lines represent boundaries of lithostratigraphic units. In the lithological description, C stands for clay, Si for silt, S for sand and Gy for gyttja. Undulating horizontal lines mark sharp/erosional lithological contacts. Also shown is the position of the IRSL samples for comparison with sediment moisture.

pinpoints the presence of the tephra, but this (magnetic) signal is not indicative, as investigation of several of these coarse-grained layers with high susceptibility values did not yield any tephra finds.

The tephra itself is composed of about 80% vitreous material, which is angular to subrounded in morphology and contains a number of vesicles and inclusions. Microscoriae and micropumices are also found within the sample (Fig. 2A). Grain-size analysis on the bulk tephra shows a two-modal distribution, with a peak around 63 μ m and a broader peak centred on 100–150 μ m (Fig. 2B). However, optical investigation of the magnetically separated fractions indicated that the peak at 63 μ m relates exclusively to rounded particles of quartz and feldspar. We interpret this fraction as aeolian fine sands–silts in accordance with de Beaulieu & Reille (1984), who concluded that wind-transported material might represent most of the sediment accumulated in Les Echets. On the other hand, the magnetic fraction consists only of glass fragments, pumice and biotite flakes, and the grain size of shards ranges from 60 μ m to 250 μ m, with a peak around 100–150 μ m (Fig. 2). Other magmatic minerals found in association with the tephra include rare olivines, clinopyroxenes and brown amphiboles (hornblende type) partially or completely enclosed in glass.

Twenty shards from the horizon at 10.86 m in EC 3 were analysed by electron microprobe and the major element results place this tephra among the basanites/tephrites field, very close to the foidites, as indicated by the SiO₂ concentrations of *c.* 43.9% and a total alkali concentration of 7.8% (Fig. 2C). Some other distinctive geochemical characteristics of this tephra include relatively high concentrations of MgO (4.85%), CaO concentrations of *c.* 11%, relatively high K₂O values in excess of 2.4% (Fig. 2C, Table 1) and high P₂O₅ (*c.* 1%) values.

Several other potential tephra horizons have also been identified within the Les Echets sequences, but obtaining geochemical data has proved difficult because of the low concentration of shards present. Further work is currently ongoing to characterize these horizons and will be reported at a later stage.

Age and possible origin of the tephra

Despite the large standard deviations, the IRSL age estimates provide some chronological age control and suggest that the sediment sequence presented here is of MIS 3 age (Fig. 3). The two IRSL dates near the bottom of the sequence gave ages of late MIS 5–MIS 4, in

Table 3. Summary of luminescence data including sampled core depth, concentration of dose rate relevant elements (K, Th, U), measured sediment moisture (W), dose rate (D), equivalent dose (D_e) and resulting IRSL ages.

| Sample (kyr) | Depth (cm) | K (%) | Th (ppm) | U (ppm) | W (%) | D (Gy kyr ⁻¹) | ED _{IRSL} BL (Gy) | Age _{IRSL} BL (kyr) |
|--------------|------------|-----------|------------|-----------|-------|---------------------------|----------------------------|------------------------------|
| LE3-2k | 431–437 | 1.48±0.13 | 14.94±0.31 | 3.27±0.14 | 35.2 | 3.53±0.29 | 73.4±1.1 | 20.8±1.8 |
| LE3-3k | 554–558 | 1.44±0.13 | 13.07±0.27 | 3.28±0.14 | 41.6 | 3.15±0.26 | 72.6±1.0 | 23.0±1.9 |
| LE3-7k | 775–780 | 1.53±0.14 | 11.27±0.24 | 3.40±0.15 | 52.1 | 2.85±0.23 | 92.1±2.3 | 32.4±2.8 |
| LE3-9m | 893–898 | 1.36±0.12 | 9.08±0.21 | 2.57±0.11 | 58.0 | 2.24±0.18 | 76.2±1.4 | 34.0±2.8 |
| LE3-11k | 1050–1055 | 1.57±0.14 | 11.66±0.24 | 2.96±0.13 | 42.4 | 2.97±0.24 | 127.2±7.2 | 42.9±4.2 |
| LE3-12k | 1104–1109 | 1.71±0.15 | 11.29±0.24 | 3.02±0.13 | 48.1 | 2.92±0.23 | 125.9±1.0 | 43.2±3.4 |
| LE3-15m | 1254–1259 | 1.44±0.13 | 11.06±0.24 | 3.37±0.15 | 57.8 | 2.63±0.22 | 104.2±5.1 | 40.0±3.8 |
| LE3-19k | 1413–1418 | 1.45±0.13 | 11.24±0.24 | 2.89±0.13 | 30.9 | 3.0±0.25 | 161.2±2.6 | 52.1±4.4 |
| LE3-22k | 1688–1693 | 1.65±0.15 | 10.63±0.22 | 3.11±0.13 | 44.5 | 2.91±0.24 | 181.7±4.4 | 62.5±5.4 |
| LE3-25k | 1867–1872 | 1.05±0.09 | 6.82±0.14 | 1.70±0.07 | 24.1 | 2.12±0.17 | 154.4±1.9 | 72.9±5.7 |

good agreement with the ages expected for these sediments based on pollen stratigraphy (Andrieu-Ponel *et al.* 2006; Veres *et al.* 2007) (Fig. 3, Table 3). The uppermost available dates would indicate that sediments around 4 m depth are of MIS 2 age.

Two IRSL samples bracket the tephra horizon at 11.09–11.04 m and 10.55–10.50 m and gave overlapping ages of 43 200±3400 yr BP (LE3-12) and 42 900±4200 yr BP (LE3-11). Considering a potential change in water content with time, the minimum IRSL age of the tephra could be about 45 000 yr BP (Fig. 3). Two ¹⁴C ages (LuS 6350 and LuS 6351) also closely bracket the tephra layer and fall within the errors of the IRSL dates. The date of 36 600±500 ¹⁴C yr BP at 10.89–10.88 m is consistent with the other ¹⁴C age determinations on macrofossils and provides a tentative ‘calibrated’ age of *c.* 41 720±310 yr BP below the tephra layer (Fig. 3, Table 2). However, sample LuS 6351 dated to 42 000±1000 ¹⁴C yr BP at 10.83–10.82 m appears to produce aberrant ages and is treated here as unreliable until supported by more age determinations. Nonetheless, we believe that the age of the tephra falls in the range 42 000–45 000 yr BP.

The high concentration of glass shards, the size of the shards and the visible nature of the tephra at 10.86 m suggested initially that this tephra originates from a proximal source in the Massif Central, *c.* 150 km to the west (Fig. 1A). The general aspect of the vitreous and other magmatic grains indicates that the mineral associations identified within this tephra might be linked to a highly explosive phreatomagmatic eruption. A number of eruptions are known to have occurred during this time in the Massif Central region (e.g. Nowell *et al.* 2006) and were associated with the initial formation of the Chaîne des Puys (Vernet *et al.* 1998). One of the phreatomagmatic phases associated with the Chaîne des Puys activity was the Puy de la Toupe eruption at *c.* 45 500 yr BP (thermoluminescence age estimate from Guérin 1983). This fits well with the age estimate for the Les Echets tephra (*c.* 42 000–45 000 yr BP); however, the basanite composition of the tephra identified at Les Echets (Fig. 2C) suggests that the origin of this tephra lies outside the Massif Central region, and may lie in-

stead in the Eifel region (*c.* 500 km to the northeast) (Fig. 1A).

A large phreatomagmatic eruption is known to have occurred in the Eifel region around 45 000 yr BP (Schmincke *in press*; or estimated to >35 000 yr BP in Zolitschka *et al.* 1995), resulting in the formation of Meerfelder Maar. However, chemical analysis of glass material from this eruption is still unavailable and so we are unable to provide a detailed geochemical comparison in this article. Nevertheless, a comparison of Les Echets tephra with averaged chemical data (XRF analyses) from 112 tuff ring, pyroclastic material and lava-flow samples from Quaternary eruptive centres from the West Eifel (Mertes 1983) indicate that this volcanic field is the most likely source for our tephra (Fig. 2C). Most of the samples from the Eifel cluster at the border between basanites and foidites – compositions that are similar to the Les Echets tephra. In contrast, chemical data from 17 glass-pyroclastic samples from the Chaîne des Puys, Massif Central (Vernet *et al.* 1998), show that materials from this volcanic field, ranging from trachy-basalts to trachytes, are of a different composition to the Les Echets tephra. Consequently, we believe that the West Eifel volcanic field is the most likely origin of the Les Echets tephra. Up until now, however, no other tephra of similar composition and age to the Les Echets tephra has been reported in other sequences spanning the last glacial period. If this tephra originates from the Eifel region, its presence at Les Echets may indicate that it was widely distributed in western and central Europe and highlights the possibility of this event being traced within other long-core or loess sequences (Fig. 1A). Indeed, there would be great potential in tracing this event within some of the maar sequences in the Eifel region itself (Sirocko *et al.* 2005) as well as within the French sequences, e.g. Grande Pile (Woillard & Mook 1982) or the Velay sites (de Beaulieu & Reille 1992), and even in some of the key laminated sequences in Italy (e.g. Allen *et al.* 1999). Thus, it may be possible to utilize this tephra as a tie-point for palaeorecords spanning the last glacial period in Europe.

The potential of using this tephra as a marker horizon, however, depends entirely on whether it can be

identified in other palaeoarchives. Indeed, one peculiarity of this work is that the entire EC 1 sequence spanning MIS 3 and MIS 2 (*c.* 40 m) has been screened for the presence of tephra shards, and no similar shards were identified. This may be a reflection of the operation of complex sedimentary processes in the basin resulting in an uneven distribution of tephra, which has been observed within other lacustrine environments (e.g. Mangerud *et al.* 1984; Davies *et al.* 2001; Pyne O'Donnell 2007). If so, there is a possibility that this tephra is present in cryptotephra from within EC 1, but the extensive nature of the mineral material precludes the isolation and extraction of volcanic particles. On the other hand, core EC 1 has been dated at high resolution and the results indicate that sediments >36 700 yr BP have been seriously disturbed by erosive processes (Wohlfarth *et al.* in press). The age estimates available for core EC 3 and the identification of this visible tephra layer validate the inter-core correlation suggested in Veres *et al.* (2007), where only subunit G₃ from core EC 3 could be related to core EC 1 (the whole of unit G). It is therefore likely that subunits G₁–G₂ are not recorded in core EC 1, and that core EC 3 although recovered from a more littoral area is more complete, highlighting the complex nature of sedimentation and sediment preservation in this large, glacially formed lacustrine basin (Fig. 1B).

Evidence for DO climate variability in relation to the Les Echets tephra horizon

The Les Echets tephra horizon falls in the interval of recurrent variations in organic matter content in unit G, which according to our chronology is coeval with MIS 3 (Figs 3, 4). These fluctuations in organic matter are similar in appearance to the temperature variations (DO events) identified in the Greenland ice-core records (Meese *et al.* 1997; Johnsen *et al.* 2001) (Fig. 3). Indeed, the multiproxy investigation of the parallel sequence EC 1 (Veres 2007; Wohlfarth *et al.* in press) interpreted similar quasi-cyclic lithological variations between organic-rich silty gyttja layers and inorganic layers to represent the response of the lake system to DO climate variability. Intervals with higher organic matter content identified in core EC 1, similar to the ones described here (see Veres *et al.* 2007), are interpreted as periods of higher lake organic primary productivity and interstadial conditions. Stadial conditions, on the other hand, are marked by an increase in mineral content, high magnetic susceptibilities and bulk densities. Hence, it is reasonable to assume that the marked lithological fluctuations seen in core EC 3 are responses to the same millennial-scale climatic events (Figs 3, 4).

The two most distinct organic horizons are present within unit G₁, prior to the deposition of the tephra horizon, and according to our chronological model this

unit was deposited in early MIS 3 (Fig. 3). Although the timing of the two large organic matter peaks cannot be constrained with the available chronological data, it is possible that they relate to DO 12 and 14 (Fig. 3). These early MIS 3 (>40 000 yr BP) interstadial events are of considerable length in the Greenland ice-cores (Meese *et al.* 1997; Johnsen *et al.* 2001), and the distinct organic-rich layers may indicate that they relate either to environmental conditions which favoured high organic matter production or to long periods of organic accumulation in the basin.

If the large organic matter peak at 11.70–11.24 m depth relates to DO 12, as suggested in Fig. 5, then it is possible that the three minor increases in organic matter content in subunit G₂ could represent the sequence of shorter interstadial events subsequent to DO 12 in the ice-cores (Fig. 3). By taking account of the IRSL ages that bracket the tephra horizon, it appears that the tephra layer could have been deposited some time during the interval between DO 12 and DO 8 (Figs 3, 5). More specifically, the tephra layer falls in association with the peak in organic matter (the first of the three minor peaks) from subunit G₂, which could, if our assumptions are correct, relate to DO 11 (Fig. 5), which is dated to *c.* 43 500–42 500 yr BP on the GRIP ss09sea time scale (Johnsen *et al.* 2001). Although the correlations above should be regarded as tentative, the ages obtained for the tephra layer and the onset of subunit G₂

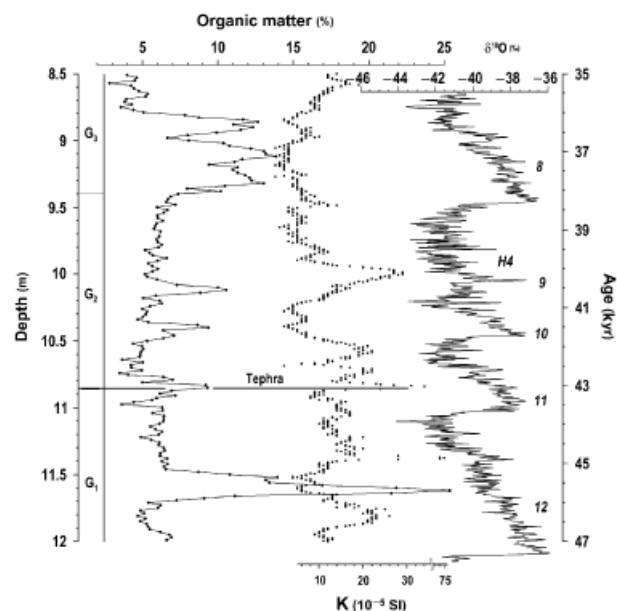


Fig. 5. Comparison of the sediment organic matter content and magnetic susceptibility data between 12.00 and 8.50 m depth in core EC 3 and the GRIP isotopic record spanning the time interval between 47 and 35 kyr BP (Johnsen *et al.* 2001). Numbers 9–12 refer to DO events, and H4 stands for Heinrich event 4. The suggested correlations are only tentative due to the chronological limitations, but it is possible that the tephra layer shown by the vertical line was deposited during DO interstadial 11. Note the scale difference between graphs.

are in good agreement with the ice-core data (Fig. 3). Our correlations raise the possibility of narrowing the search for a corresponding ash-fall event in other records for the period within and immediately around this event (Fig. 5). Moreover, the significant rise in susceptibility values after the uppermost organic layer within subunit G₂ corresponding to high dry densities and a coarsening of the grain size point towards an erosional event in the catchment area (Fig. 4). This interval may relate to the long stadial between DO 9 and DO 8, a time-interval also characterized by the deposition of Heinrich layer 4 in the nearby Atlantic Ocean (Hemming 2004) (Fig. 5).

Above this interval (<9.46 m depth), several more clearly delimited intervals with increasing organic matter contents contrast markedly with intervening intervals with increasing susceptibilities and dry densities (Figs 3, 4). It is likely that these rapid quasi-cyclic lithological changes represent the response of the lake system to the short interstadials/stadials that characterized late MIS 3 (i.e. subsequent to Heinrich event 4).

Conclusions

The Les Echets tephra (c. 42 000–45 000 yr BP) provides new evidence of a past volcanic event in central Europe. We propose that the Eifel region is the most likely source of this tephra, which falls within MIS 3 and was deposited during a small interstadial event, possibly relating to DO 11 in the North Atlantic. As such, this tephra may potentially act as a time-synchronous marker horizon for deposits of middle MIS 3 age to better assess the regional development and environmental response of DO events in the terrestrial environments of central-western Europe. Further work is required to identify this tephra in other terrestrial deposits, to explore its full distribution pattern and to determine the potential for using this horizon as a time-parallel marker for precise correlation of different palaeoarchives.

Acknowledgements. – We thank Peter Hill (University of Edinburgh), André Poulet, Didier Kéravis, Elisabeth Lallier-Vergès (University of Orléans) and Hans-Ulrich Schmincke (Geomar Kiel) for assistance with tephra analysis and interpretation. Comments by John Pilcher and Christel van den Bogaard greatly improved the manuscript. Siwan Davies acknowledges support from the Quaternary Research Association and the Nuffield Foundation NAL/01110/G. Barbara Wohlfarth acknowledges financial support from the Swedish Research Council. This is a contribution to the ESF EuroCores on EuroCLIMATE project RESOLuTION.

References

Adamiec, G. & Aitken, M. J. 1998: Dose-rate conversion factors: An update. *Ancient TL* 16, 17–30.
 Allen, J. R. M., Brandt, U., Brauer, A., Hubberten, H.-W., Huntley, B., Keller, J., Kraml, M., Mackensen, A., Mingram, J., Negendank, J. F. W., Nowaczyk, N. R., Oberhansli, H., Watts, W. A., Wulf, S.

& Zolitschka, B. 1999: Rapid environmental changes in southern Europe during the last glacial period. *Nature* 400, 740–743.
 Andrieu-Ponel, V., de Beaulieu, J.-L., Cheddadi, R., Dubois, J. M., Gandouin, E., Guiter, F., Kéravis, D., Kukla, G., Lallier-Vergès, E., Ponel, P., Thouveny, N., Veres, D. & Wohlfarth, B. 2006: Analyse multidisciplinaire de la nouvelle séquence climatique (EC1) du marais des Echets (alt.: 267 m, Ain, France). *Rapport D2 C.CC.ASMG.03-012/A de l'ANDRA*, 173 pp.
 Blockley, S. P. E., Lane, C. S., Lotter, A. F. & Pollard, A. M. 2007: Evidence for the presence of the Vedde Ash in Central Europe. *Quaternary Science Reviews* 26, 3030–3036.
 Dansgaard, W., Johnson, S. J., Clausen, H. B., Dahljensen, D., Gundestrup, N. S., Hammer, C. U., Hvidbjerg, C. S., Steffensen, J. P., Sveinbjörnsdóttir, A. E., Jouzel, J. & Bond, G. 1993: Evidence for general instability of past climate from a 250-kyr ice-core record. *Nature* 364, 218–220.
 Davies, S. M., Turney, C. S. M. & Lowe, J. J. 2001: Identification and significance of a visible, basalt-rich Vedde Ash layer in a Late-glacial sequence on the Isle of Skye, Inner Hebrides, Scotland. *Journal of Quaternary Science* 16, 99–104.
 Davies, S. M., Wastegård, S. & Wohlfarth, B. 2003: Extending the limits of the Borrobol Tephra to Scandinavia and detection of new early Holocene tephra. *Quaternary Research* 59, 345–352.
 Davies, S. M., Hoek, W. Z., Bohncke, S. J. P., Lowe, J. J., Pyne O'Donnell, S. & Turney, C. S. M. 2005: Detection of Lateglacial distal tephra layers in the Netherlands. *Boreas* 34, 123–135.
 de Beaulieu, J.-L. & Reille, M. 1984: A long Upper Pleistocene pollen record from Les Echets, near Lyon, France. *Boreas* 13, 111–132.
 de Beaulieu, J.-L. & Reille, M. 1992: The last climatic cycle at La Grande Pile (Vosges, France): A new pollen profile. *Quaternary Science Reviews* 11, 431–438.
 Fairbanks, R. G., Mortlock, R. A., Chiu, T.-C., Cao, L., Kaplan, L. A., Guilderson, T. P., Fairbanks, T. W., Bloom, A. L., Grootes, P. M. & Nadeau, M.-J. 2005: Radiocarbon calibration curve spanning 0 to 50,000 years BP based on paired ²³⁰Th/²³⁴U/²³⁸U and ¹⁴C dates on pristine corals. *Quaternary Science Reviews* 24, 1781–1796.
 Genty, D., Blamart, D., Ouahdi, R., Gilmour, M., Baker, A., Jouzel, J. & Van-Exter, S. 2003: Precise dating of Dansgaard-Oeschger climate oscillations in western Europe from stalagmite data. *Nature* 421, 833–837.
 Guérin, G. 1983: *La thermoluminescence des plagioclases, method de datation du volcanisme. Applications au domaine volcanique francais: Chaîne des Puys, Mont Dore et Cezallier, Bas Vivarais*. Ph.D. dissertation, Université Paris-6, 258 pp.
 Hang, T., Wastegård, S., Veski, S. & Heinsalu, A. 2006: First discovery of cryptotephra in Holocene peat deposits of Estonia, eastern Baltic. *Boreas* 35, 644–649.
 Heiri, O., Lotter, A. F. & Lemcke, G. 2001: Loss on ignition as a method for estimating organic and carbonate content in sediments: Reproducibility and comparability of results. *Journal of Paleolimnology* 25, 101–110.
 Hemming, S. R. 2004: Heinrich events: Massive late Pleistocene detritus layers of the North Atlantic and their global climate imprint. *Review of Geophysics* 42, doi: 10.1029/2003RG000128.
 Johnsen, S. J., Clausen, H. B., Dansgaard, W., Fuhrer, K., Gundestrup, N., Hammer, C. U., Iverson, P., Jouzel, J., Stauffer, B. & Steffensen, J. P. 1992: Irregular glacial interstadials recorded in a new Greenland ice core. *Nature* 363, 311–313.
 Johnsen, S. J., Dahl-Jensen, D., Gundestrup, N., Steffensen, J. P., Clausen, H. B., Miller, H., Mason-Delmotte, V., Sveinbjörnsdóttir, A. E. & White, J. 2001: Oxygen isotope and palaeotemperature records from six Greenland ice-core stations: Camp Century, Dye-3, GRIP, GISP2, Renland and NorthGRIP. *Journal of Quaternary Science* 16, 299–307.
 Juschus, O., Preusser, F., Melles, M. & Radtke, U. 2007: Applying SAR-IRSL methodology for dating fine-grain sediments from Lake El'gygytgyn, northeastern Siberia. *Quaternary Geochronology* 2, 187–194.
 Klasen, N., Preusser, F., Fiebig, M., Blei, A. & Radtke, U. 2006: Luminescence properties of glaciofluvial sediments from the Bavarian Alpine Foreland. *Radiation Measurements* 41, 866–870.

- Konert, M. & Vandenberghe, J. 1997: Comparison of laser grain size analysis with pipette and sieve analysis: A solution for the underestimation of the clay fraction. *Sedimentology* 44, 523–535.
- Lang, A. & Zolitschka, B. 2001: Optical dating of annually laminated lake sediments: A test case from Holzmaar/Germany. *Quaternary Science Reviews* 20, 737–742.
- Le Bas, M. L., Le Maitre, R. W., Streckeisen, A. & Zanettin, B. 1986: A chemical classification of volcanic rocks based on the total alkali-silica diagram. *Journal of Petrology* 27, 745–750.
- Mackie, E. A. V., Davies, S. M., Turney, C. S. M., Dobbyn, K., Lowe, J. J. & Hill, P. G. 2002: The use of magnetic separation techniques to detect basaltic microtephra in last glacial–interglacial transition (LGIT: 15–10 ka cal BP) sediment sequences in Scotland. *Scottish Journal of Geology* 38, 21–30.
- Mangerud, J., Lie, S. E., Furnes, H., Kristiansen, I. L. & Lomo, L. 1984: A Younger Dryas ash bed in Western Norway, its possible correlations with tephra in cores from the Norwegian Sea and the North Atlantic. *Quaternary Research* 21, 85–104.
- Meese, D. A., Gow, A. J., Alley, R. B., Zielinski, G. A., Grootes, P. M., Ram, M., Taylor, K. C., Mayewski, P. A. & Bolzan, J. F. 1997: The Greenland Ice Sheet Project 2 depth-age scale: Methods and results. *Journal of Geophysical Research* 102, 26411–26423.
- Mertes, H. 1983: Aufbau und Genese des Westeifel Vulkanfelds. *Bochumer Geologische und Geotechnische Arbeiten* 9, 415 pp.
- Nowell, D. A. G., Jones, C. M. & Pyle, D. M. 2006: Episodic Quaternary volcanism in France and Germany. *Journal of Quaternary Science* 21, 645–675.
- Pouchou, J. & Pichoir, F. 1991: Quantitative analysis of homogenous or stratified microvolumes applying the model 'PAP'. In Heinrich, K. F. J. & Newbury, D. E. (eds.): *Electron Probe Quantitation*, 31–75. Plenum Press, New York.
- Prescott, J. R. & Hutton, J. T. 1994: Cosmic ray contributions to dose rates for luminescence and ESR dating: Large depth and long time variations. *Radiation Measurements* 23, 497–500.
- Preusser, F. 1999: Lumineszenzdatierung fluviatiler Sedimente – Fallbeispiele aus der Schweiz und Norddeutschland. *Kölner Forum für Geologie und Paläontologie* 3, 63 pp.
- Preusser, F. 2003: IRSL dating of K-rich feldspars using the SAR protocol: Comparison with independent age control. *Ancient TL* 21, 17–23.
- Preusser, F. & Kasper, H. U. 2001: Comparison of dose rate determination using high-resolution gamma spectrometry and inductively coupled plasma-mass spectrometry. *Ancient TL* 19, 17–21.
- Preusser, F., Geyh, M. A. & Schlüchter, C. 2003: Timing of Late Pleistocene climate change in lowland Switzerland. *Quaternary Science Reviews* 22, 1435–1445.
- Preusser, F. & Schlüchter, C. 2004: Dates from an important early Late Pleistocene ice advance in the Aare Valley, Switzerland. *Eclogae Geologicae Helveticae* 97, 245–253.
- Preusser, F., Drescher-Schneider, R., Fiebig, M. & Schlüchter, C. 2005: Re-interpretation of the Meikirch pollen record, Swiss Alpine Foreland, and implications for Middle Pleistocene chronostratigraphy. *Journal of Quaternary Science* 20, 607–620.
- Preusser, F., Ramseyer, K. & Schlüchter, C. 2006: Characterisation of low luminescence intensity quartz from Westland, New Zealand. *Radiation Measurements* 41, 871–877.
- Pyle, D. M., Ricketts, G. D., Margari, V., van Andel, T. H., Sinitsyn, A. A., Praslov, N. D. & Lisitsyn, S. 2006: Wide dispersal and deposition of distal tephra during the Pleistocene 'Campanian Ignimbrite/Y5' eruption, Italy. *Quaternary Science Reviews* 25, 2713–2728.
- Pyne-O'Donnell, S. D. F. 2007: Three new distal tephra in sediments spanning the Last Glacial–Interglacial transition in Scotland. *Journal of Quaternary Science* 22, 559–570.
- Reimer, P. J., Baillie, M. G. L., Bard, E., Bayliss, A., Beck, J. W., Bertrand, C. J. H., Blackwell, P. G., Buck, C. E., Burr, G. S., Cutler, K. B., Damon, P. E., Edwards, R. L., Fairbanks, R. G., Friedrich, M., Guilderson, T. P., Hogg, A. G., Hughen, K. A., Kromer, B., McCormac, F. G., Manning, S. W., Ramsey, C. B., Reimer, R., Remmele, S., Southon, J. R., Stuiver, M., Talamo, S., Taylor, F. W., van der Plicht, J. & Weyhenmeyer, C. E. 2004: IntCal04 terrestrial radiocarbon age calibration, 26–0 ka BP. *Radiocarbon* 46, 1029–1058.
- Rose, N. L., Golding, P. N. E. & Battarbee, R. W. 1996: Selective concentration and enumeration of tephra shards from lake sediment cores. *Holocene* 6, 243–246.
- Sánchez Goñi, M. F., Cacho, I., Turon, J. -L., Guiot, J., Sierro, F. J., Peyrouquet, J.-P., Grimalt, J. O. & Shackleton, N. J. 2002: Synchronicity between marine and terrestrial responses to millennial scale climatic variability during the last glacial period in the Mediterranean region. *Climate Dynamics* 19, 95–105.
- Schmincke, H.-U. In press: Quaternary volcanism of the East and West Eifel (Central Europe). In McCann, T. (ed.): *Geology of Central Europe*. Geological Society of London.
- Sirocko, F., Seelos, K., Schaber, K., Rein, B., Dreher, F., Diehl, M., Lehne, R., Jäger, K., Krbetschek, M. & Degering, D. 2005: A late Eemian aridity pulse in central Europe during the last glacial inception. *Nature* 436, 833–836.
- Spötl, C. & Mangini, A. 2002: Stalagmite from the Austrian Alps reveals Dansgaard–Oeschger events during isotope stage 3: Implications for the absolute chronology of Greenland ice cores. *Earth and Planetary Science Letters* 203, 507–518.
- Thomas, P. J., Murray, A. S. & Sandgren, P. 2003: Age limit and age underestimation using different OSL models from lacustrine quartz and polymineral fine grains. *Quaternary Science Reviews* 22, 1139–1143.
- Turney, C. S. M. 1998: Extraction of rhyolitic ash from minerogenic lake sediments. *Journal of Paleolimnology* 19, 199–206.
- Vandergoes, M., Newnham, R., Preusser, F., Hendy, C., Lowell, T., Fitzsimons, S., Hogg, A., Kasper, H. U. & Schlüchter, C. 2005: Southern Ocean terrestrial record showing local modification of glacial–interglacial climate signals. *Nature* 436, 242–245.
- van der Plicht, J., Beck, J. W., Bard, E., Baillie, M. G. L., Blackwell, P. G., Buck, C. E., Friedrich, M., Guilderson, T. P., Hughen, K. A., Kromer, B., McCormac, F. G., Bronk Ramsey, C., Reimer, P. J., Reimer, R. W., Remmele, S., Richards, D. A., Southon, J. R., Stuiver, M. & Weyhenmeyer, C. E. 2004: Notcal04-Comparison/calibration ¹⁴C records 26–50 cal kyr BP. *Radiocarbon* 48, 1–14.
- Veres, D., Wohlfarth, B., Andrieu-Ponel, V., Björck, S., de Beaulieu, J.-L., Digerfeldt, G., Ponel, P., Ampel, L., Davies, S., Gaudouin, E. & Belmecheri, S. 2007: The lithostratigraphy of the Les Echets basin, France: Tentative correlation between cores. *Boreas* 36, 326–340.
- Veres, D. 2007: *Terrestrial Response to Dansgaard–Oeschger Cycles and Heinrich Events During MIS 3 and 2. The Lacustrine Record of Les Echets, France*. Ph.D. dissertation, Stockholm University, 128 pp.
- Vernet, G., Raynal, J. P., Fain, J., Miallier, D., Montret, M., Pilleyre, T. & Sanzelle, S. 1998: Tephrostratigraphy of the last 160 ka in western Limagne (France). *Quaternary International* 47–48, 139–146.
- Wohlfarth, B., Veres, D., Ampel, L., Lacourse, T., Blaauw, M., Preusser, F., Andrieu-Ponel, V., Kéravis, D., Lallier-Vergès, E., Björck, S., Davies, S., de Beaulieu, J.-L., Risberg, J., Hormes, A., Kasper, H. U., Possnert, G., Reille, M., Thouveny, N. & Zander, A. In Press: Rapid ecosystem response to abrupt climate changes during the last glacial period in Western Europe 40–16 kyr BP. *Geology*.
- Woillard, G. M. & Mook, W. G. 1982: Carbon-14 dates at Grande Pile: Correlation of land and sea chronologies. *Science* 215, 159–161.
- Zolitschka, B., Negendank, J. F. W. & Lottermoser, B. G. 1995: Sedimentological proof and dating of the early Holocene volcanic eruption of Ulmener Maar (Vulkaneifel, Germany). *Geologische Rundschau* 84, 213–219.